Progress in Reaction Kinetics and Mechanism

ARTICLE

Open Access

https://doi.org/10.48130/prkm-0026-0015

Progress in Reaction Kinetics and Mechanism **2026**, 51: e021

Kinetic insights into component-governed pyrolysis mechanisms and synergistic effects of coconut wastes

Qiang Yu[1], Zihao Li[1,2], Rui Shan[2,3], Chengyu Li[2,3*], Jun Zhang[2,3*] and Haoran Yuan[2,3]

[1] *College of Information and Electrical Engineering, China Agricultural University, Beijing 100083, China*
[2] *Guangzhou Institute of Energy Conversion, Chinese Academy of Sciences (CAS), Guangzhou 510640, China*
[3] *Guangdong Provincial Key Laboratory of High-Quality Recycling of End-of-Life New Energy Devices, Guangzhou 510640, China*
* Correspondence: licy@ms.giec.ac.cn (Li C); zhangjun@ms.giec.ac.cn (Zhang J)

Abstract

This study presents a comprehensive mechanistic investigation into the pyrolysis behaviors of three coconut waste components (coconut shell, coir, and husk) by integrating Py-GC/MS and a developed Gaussian fit-isoconversional kinetic method. A four-independent-parallel-reaction model based on combined water, hemicellulose, cellulose, and lignin was established, accurately simulating the pyrolysis process with high-fitting correlation coefficients. Product analysis revealed distinct pathways: coconut coir, rich in cellulose, exhibited exceptional selectivity toward furans, while coconut shell and husk, with higher hemicellulose content, favored acid and phenolic production, respectively, strongly influenced by their specific lignin types. Kinetic analysis quantitatively demonstrated that *in-situ* released acetic acid from hemicellulose autocatalytically reduced its decomposition activation energy. Furthermore, the activation energy for lignin pyrolysis in all samples was significantly lower than that of isolated lignin, highlighting catalytic synergy from surrounding carbohydrates. This work provides fundamental insights into composition-dependent reaction mechanisms and offers a strategic basis for the targeted valorization of lignocellulosic wastes into specific bio-based chemicals.

Keywords: Coconut waste, Pyrolysis, Kinetic analysis, Isoconversional method

Citation: Yu Q, Li Z, Shan R, Li C, Zhang J, et al. 2026. Kinetic insights into component-governed pyrolysis mechanisms and synergistic effects of coconut wastes. *Progress in Reaction Kinetics and Mechanism* 51: e021 https://doi.org/10.48130/prkm-0026-0015

Introduction

As the energy crisis continues to intensify, countries around the globe are placing increasing emphasis on the development and utilisation of renewable energy sources[1]. Biomass accounts for about 12.83% of the environmental renewable energy stock, and its utilisation is expected to span the coming decades[2]. Coconut residue wastes are among the most abundant biomass resources worldwide, with a global production of 62.5 million tonnes per year. Coconut residue is one of the most abundant biomass resources worldwide, with a global production of 62.5 million tonnes per year[3]. As a typical carbon-rich biomass, it is usually disposed of by landfilling and incineration, which not only causes serious environmental pollution but also leads to a waste of resources[4]. It is worth noting that these coconut residues primarily consist of the endocarp (coconut husks), the mesocarp (coconut coir), and the epicarp (coconut shells). Among these, coconut husks and shells are rich in hemicellulose and lignin, while coconut coir is rich in cellulose[5]. All these components possess high calorific values. Therefore, the rational development and utilisation of coconut residue is of great significance.

Pyrolysis is a thermochemical conversion route in which biomass is decomposed under oxygen-deficient conditions to generate biochar, condensable liquids, and permanent gases[6]. Compared to other thermal or biological conversion technologies such as gasification, combustion, fermentation, and digestion[7], the main advantages of pyrolysis are converting solid biomass into solid char, the synthesis of gas/liquid fuels, facilitating fuel transportation, and meeting the market's diverse energy needs[8]. Therefore, pyrolysis technology has emerged as one of the most promising methods in the field of biomass waste disposal. The high carbon content and unique physicochemical properties of coconut residues make them excellent raw materials for producing biochar and pyrolytic gas. Sarkar & Wang[9] pyrolyzed coconut residue at temperatures ranging from 400 to 800 °C, obtaining porous biochar products yielding approximately 27~34 wt%. Millán et al.[10] gasified coconut residue in a fluidized bed reactor to produce pyrolytic gas composed of carbon monoxide, hydrogen, and methane, with a biochar by-product yield of about 13 wt%. These studies indicate that considerable attention has been paid to the thermochemical conversion of coconut residues for producing carbon materials and gaseous fuels.

In recent years, increasing attention has also been paid to the kinetic analysis of biomass pyrolysis. Model-free isoconversional methods, such as the Flynn-Wall-Ozawa (FWO), and the Kissinger-Akahira-Sunose (KAS), have been widely employed to evaluate the apparent activation energy of complex lignocellulosic materials without assuming a predefined reaction model, whereas model-based approaches, such as the distributed activation energy model (DAEM), are often used to describe the multi-step decomposition behavior of biomass and its major components. Recent studies have shown that the complementary use of model-free and model-fitting approaches can provide deeper insight into biomass thermal conversion behavior[11], while Thermogravimetric Analysis–Fourier Transform Infrared Spectroscopy (TGA-FTIR) and Pyrolyzer-Gas Chromatography/Mass Spectrometry (Py-GC/MS) combined with kinetic analysis are also effective for clarifying the pyrolysis characteristics of lignin-rich materials[12]. Nevertheless, for heterogeneous biomass systems with strongly overlapped component reactions, further component-resolved kinetic analysis is still needed. Notably, Kazawadi et al.[13] also used the distributed activation energy model (DAEM) to reveal the kinetic variations in reaction performance at

© The Author(s)

https://doi.org/10.48130/prkm-0026-0015

different stages during coconut shell pyrolysis. However, research on the product-distribution patterns and pyrolysis conversion mechanisms of bio-oil, which is a major product of coconut-residue pyrolysis (accounting for about 47–49 wt%), remains scarce[9]. Furthermore, the pyrolysis kinetics of coconut residues with different compositions still require in-depth study to better reveal their reaction mechanisms, thereby enabling product prediction and process optimization.

Inspired by the aforementioned research, this study investigates the pyrolysis behaviors of three coconut waste components, namely coconut shell, coir, and husk. Fast pyrolysis experiments were conducted using Py-GC/MS to analyze the distribution patterns of pyrolytic bio-oil products and to elucidate the conversion characteristics of the three feedstocks. In addition, non-isothermal pyrolysis experiments were performed using TG-MS, and an in-depth kinetic analysis was carried out by combining a four-independent-parallel reaction model with the isoconversional method. Particular attention was paid to the pyrolysis kinetics of the key components, namely, combined water, hemicellulose, cellulose, and lignin, as well as to the synergistic interactions among them.

Accordingly, the present work aims to address two key scientific questions: first, how the compositional differences among coconut shell, coir, and husk govern their pyrolysis pathways and product selectivity; and second, how a Gaussian fit–isoconversional strategy can be used to resolve component-level kinetic behavior and reveal synergistic effects during pyrolysis. By integrating TG-MS, Py-GC/MS, Gaussian deconvolution, and isoconversional analysis, this study provides a clearer mechanistic interpretation of composition-dependent pyrolysis behavior and offers a basis for the targeted valorization of coconut wastes.

Experiments

Materials

The endocarp (En, coconut shells), mesocarp (Me, coconut coirs), and epicarp (Ep, coconut husks) of coconuts grown in Hainan, China, were utilized as raw materials. To minimize source-related variability and focus on the intrinsic differences among the three coconut fractions, all samples used in this study were collected from the same producing region and subjected to identical pretreatment procedures. Initially, each component was separated and washed with deionized water, then dried in a 105 °C oven for 24 h. The experimental samples were ultimately prepared through grinding and sieving. Figure 1 displays the morphology of En, Me, Ep powders, and the raw material. The elemental composition analysis and industrial analysis results of the samples are detailed in Supplementary Table S1.

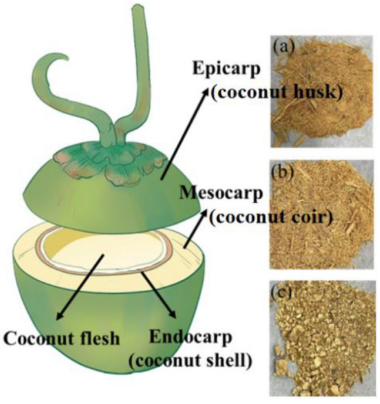

Fig. 1 Schematic diagram of coconut residues: (a) En, (b) Me, (c) Ep.

TG-MS experiments

To monitor the devolatilization process of coconut residues, the mass loss phenomenon was meticulously observed, coupled with the identification of key volatile compounds and their respective temperature ranges of release[14]. The experimental procedures were conducted utilizing a highly precise German Netzsch STA449F3 Thermogravimetric Mass Spectrometer (TG-MS). The experimental protocol entailed an initial step of weighing a 10 mg sample utilizing a differential thermal balance. Subsequently, the sample was meticulously positioned within an alumina crucible and subjected to heating up to 900 °C, employing a gradual ramp rate of 2.5, 5, 7.5, or 10 °C/min. High-purity Ar gas was employed as the carrier gas with a consistent flow rate of 50 mL/min throughout the experimental procedure.

Py-GC/MS experiments

Pyrolyzer-Gas Chromatography/Mass Spectrometry (Py-GC/MS) was employed to investigate the components generated from the pyrolysis of coconut residues. The device consisted of an analytical pyrolysis probe, CDS6200 pyrolyzer, and a 1300-ISQ7000 gas chromatograph-mass spectrometer (Thermo Fisher Scientific, USA). The experimental setup involved loading 0.2 mg of raw material into the pyrolysis tube and pyrolyzing it at the selected final temperatures. The volatile products were then analyzed with He as the carrier gas at a flow rate of 1 mL/min. Chromatographic separation was performed using a capillary column, and the chromatographic peaks were identified by referring to the NIST 20 mass spectrometry library. The selected pyrolysis temperatures were determined with reference to the thermogravimetric/differential thermogravimetric (TG/DTG) results, particularly the main DTG peak temperatures (ca. 300–330 °C) and the onset of more pronounced secondary reactions above 500 °C, in order to capture both the primary devolatilization stage and the subsequent secondary pyrolysis stage. Each Py-GC/MS experiment was replicated three times, with the relative deviation among replicate runs not exceeding 5%, to ensure the reliability of the product-distribution analysis.

Kinetic study

Kinetic models are often applied to simulate the rate of thermal degradation of raw materials or to predict the product formation rate during biomass pyrolysis. Regions with significant mass loss are usually characteristic of biomass thermal decomposition and can be represented by a global reaction (Supplementary Fig. S1a) or by independent parallel reactions of each component (P) (Supplementary Fig. S1b)[15], where VO and CA represent the generated volatile and solid components, respectively. V and S represent the volatile fraction and the fraction of solids produced by each component, respectively. Given that various coconut residues primarily consist of four major components (combined water, hemicellulose, cellulose, and lignin), a four-independent-parallel-reaction scheme is proposed to describe the pyrolysis kinetics of coconut residues.

The isoconversional method can be applied to non-isothermal data and used for the evaluation of various kinetic reactions without elucidating the reaction mechanism, predicting the apparent activation energy at asymptotically predetermined values of conversion rate[16]. The Starink method was used to calculate the activation energy with the expression shown below[17]:

$$ln\left(\frac{\beta}{T_{\alpha}^{1.92}}\right) = Const - 1.0008\frac{E_{\alpha}}{RT_{\alpha}}$$

where, β represents the heating rate, R is the universal gas constant, T is the absolute temperature (K), α represents the extent of decomposition of the material, and E_{α} refers to the activation energy (kJ/mol).

Results and discussion

TG-MS analysis

Thermal gravimetric analysis was conducted on coconut residues under four heating rates in an inert atmosphere. The TG and DTG curves for each coconut waste as a function of temperature are shown in Fig. 2.

As shown in Fig. 2, the increase in heating rate from 2.5 to 10 °C/min moved the maximum temperature of En, Me, and Ep of coconut waste from 306, 303, and 308 °C to 326, 323, and 329 °C, respectively. As the heating rate increases, the weight loss peak moves to a higher temperature. Therefore, the heating rate will affect the temperature range of pyrolysis. This change can mainly be attributed to thermal hysteresis[18].

Thermal decomposition of the pericarp manifests itself in three characteristic stages: (1) drying dehydration; (2) the release of volatiles; and (3) high-temperature carbonization. The first stage is characterized by drying/dehydration, which is mainly associated with the evaporation of free (physically adsorbed) water and the removal of weakly bound moisture. Since this stage is predominantly a physical mass-transfer process rather than the primary chemical devolatilization of biomass components, it was excluded from the kinetic model in this study, consistent with common practice reported in the literature[19]. The second stage is the release of volatile components, which is the main reaction stage of pyrolysis. Three weight-loss peaks could be observed on the DTG curves of all three feedstocks, and the temperatures corresponding to the maximum weight-loss rates were about 326, 323, and 329 °C, respectively. Three weight loss peaks could be observed on the DTG curves of all three peels, in which the peak temperatures of the largest weight loss peaks were about 326, 323, and 329 °C. The distribution of the peaks was similar for the coconut shell and husk, with the peak area increasing sequentially with increasing temperature. In contrast, the first peak area of coconut coir was significantly larger than the second peak area. During the main pyrolysis stage, the differences in DTG peak shapes among the three feedstocks can be directly related to their component distributions listed in Table 1. Coconut coir exhibits a different peak-shape pattern to coconut shell and coconut husk, which is consistent with its higher cellulose content (32.04 wt%) and lower hemicellulose content (13.91 wt%). In contrast, coconut shell and coconut husk display more similar peak shape distributions because both contain higher hemicellulose fractions (38.20 and 35.07 wt%, respectively) and comparable lignin contents (25.10 and 29.20 wt%, respectively). Since hemicellulose generally decomposes at a lower temperature than cellulose, higher hemicellulose contents contribute more strongly to the earlier DTG features, whereas the higher cellulose fraction in coconut coir enhances the main cellulose-related peak. In addition, the broad decomposition interval of lignin further contributes to peak overlap and profile broadening during the main pyrolysis stage, which is consistent with previous literature on biomass-component pyrolysis[14,20]. This stage is the active pyrolysis stage of biomass and the region with major mass loss, marking the main thermal conversion of biomass. The third stage belongs to high-temperature coke formation. The mass loss of the three peels was only 2.3%, 1.2%, and 1.8%, and the final fixed carbon content was 31.8%, 34.7%, and 32.2%, respectively. The pyrolysis process gradually slowed down at this stage. The residual biomass at this stage was finally carbonized

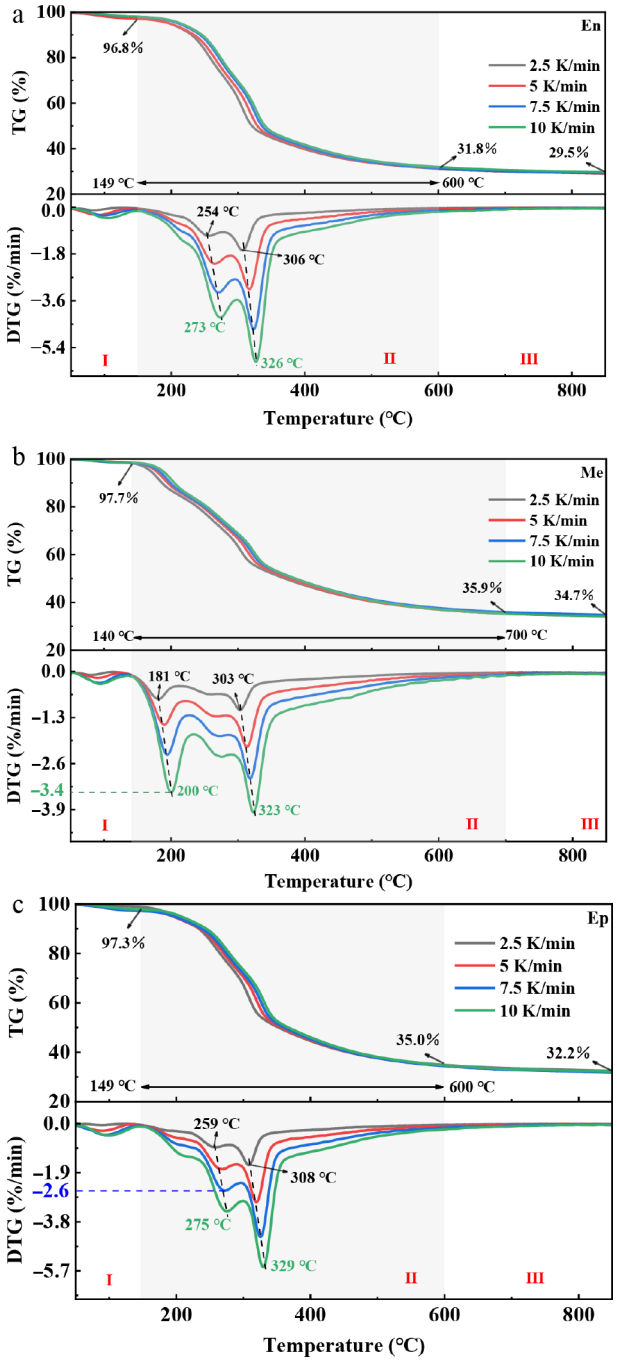

Fig. 2 TG and DTG curves of coconut wastes with different temperatures: (a) coconut shell (En), (b) coir (Me), and (c) husk (Ep).

Table 1. The comparative results of each component of coconut shell (En), coir (Me), and husk (Ep).

Sample	Combined water wt%	Hemicellulose wt%	Cellulose wt%	Lignin wt%
En	9.44	38.20	27.20	25.10
Me	24.09	13.91	32.04	29.96
Ep	8.98	35.07	26.74	29.20

https://doi.org/10.48130/prkm-0026-0015

to form stable carbon-based products mainly through condensation and rearrangement reactions[21].

Because lignocellulosic biomass consists of several thermally interacting polymeric components, its pyrolysis behavior is governed by overlapping parallel reactions rather than a single-step conversion pathway[22]. For different coconut residues, the decomposition of organic matter can be approximated by combining independent parallel reactions of components such as combined water, hemicellulose, lignin, and cellulose. The DTG curves of each component conform to the Gaussian distribution model. Based on this, the DTG curve of coconut residue was fitted to the individual behaviors of each component to reflect the overall pyrolysis behavior; the specific method is described in Supplementary Text S1. The fitting results are shown in Fig. 3. The DTG deconvolution presented in Fig. 3 was performed using the experimental DTG curve obtained at a heating rate of 7.5 K/min.

The correlation coefficients R^2 based on the fitted curves were all above 0.99, indicating the accuracy of the fitting results. In the present work, the peak widths (FWHM values) were not fixed *a priori* but were determined during the Gaussian fitting procedure to best reproduce the experimental DTG profiles. Therefore, differences in FWHM among free water, combined water, hemicellulose, cellulose, and lignin are physically reasonable because these components decompose over different temperature intervals and exhibit different degrees of peak overlap. In particular, lignin is known to decompose over a much broader temperature range than cellulose and hemicellulose, and thus a broader fitted peak width is expected. Likewise, variations in fitted FWHM among En, Me, and Ep may reflect differences in component composition, structural heterogeneity, and peak overlap. Accordingly, the FWHM values were allowed to vary among samples, since imposing identical values would improve apparent comparability at the expense of fitting fidelity and could obscure real differences in decomposition behavior. The DTG curves of the three coconut residues were deconvoluted into five independent mass loss peaks. The first peak below 150 °C corresponds to the removal of free water, which is not a primary pyrolysis stage and was therefore excluded from the kinetic model. For the subsequent volatile release stage, the four remaining mass loss peaks correspond closely to the thermal decomposition characteristics of four components—combined water, hemicellulose, cellulose, and lignin—with peak temperatures increasing in that order. For instance, the peak temperatures for these four components in coconut shell were 212.9, 273.7, 323.8, and 401.2 °C, respectively, which is consistent with findings from previous studies. It is noteworthy that the lignin component decomposes over a broad temperature range from 200 to 600 °C. This indicates that while hemicellulose and cellulose undergo thermal decomposition, the lignin component decomposes simultaneously, leading to more significant co-pyrolysis synergistic effects in these overlapping temperature regions. To compare and analyze the pyrolysis characteristics of the coconut residues, Supplementary Fig. S2 presents the independent TG/DTG curves for each component, and Table 1 lists the normalized peak area proportion for each component. The proportion indirectly reflects the proportional content of the corresponding component in the raw material. As shown in Supplementary Fig. S2 and Table 2, compared to the other two feedstocks, coconut coir exhibits a higher cellulose content and a lower hemicellulose content, which is in complete agreement with prior research. Similarly, the lignin content across the different feedstocks remains consistent.

Supplementary Fig. S3 presents the MS spectra of gaseous products from the pyrolysis of the three coconut residues. In the present study, the discussion focuses on the representative fragment ions m/z = 18, 28, and 44, corresponding to H_2O^+, CO^+, and CO_2^+, respectively. These three ions were selected because they are closely associated with the major oxygen-removal pathways during lignocellulosic biomass pyrolysis, namely dehydration, decarbonylation, and decarboxylation, and can therefore provide a direct

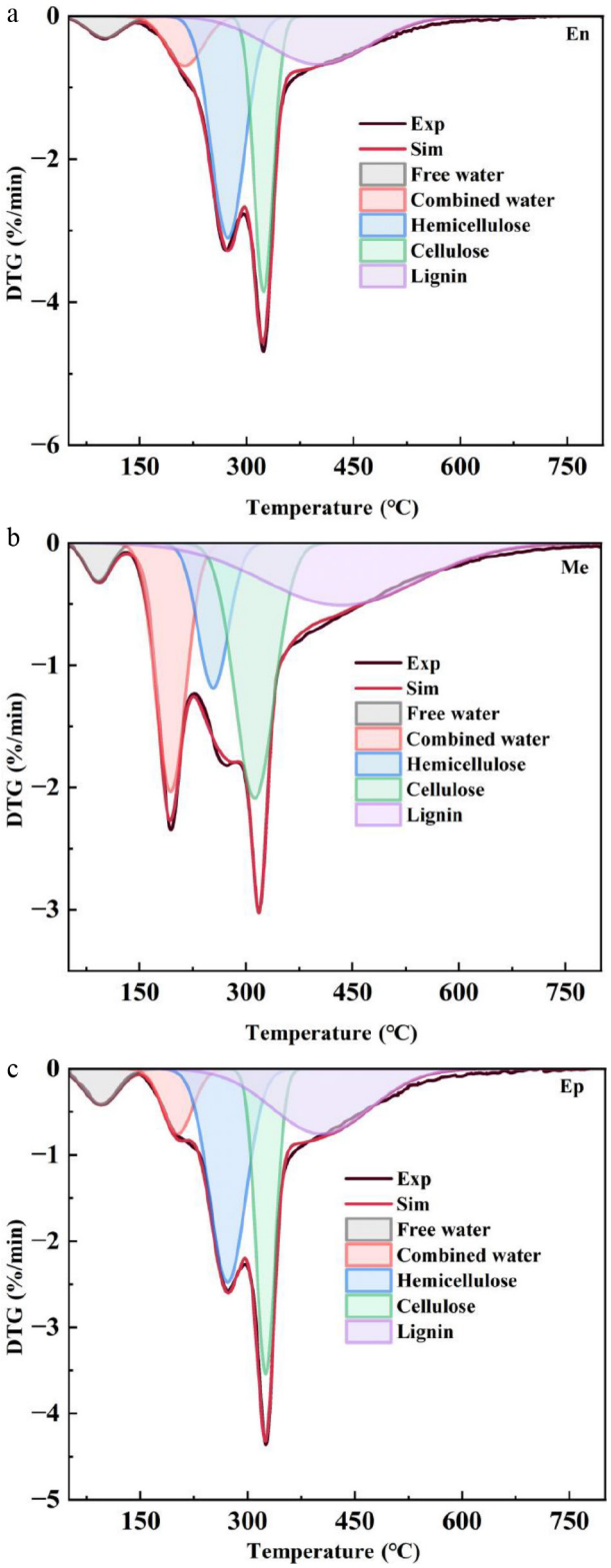

Fig. 3 Simulated DTG curves for (a) coconut shell (En), (b) coir (Me), and (c) husk (Ep).

Table 2. Total average E_a compared with the E_a of each component after deconvolution.

Sample	E_a (kJ/mol)		
	En	Me	Ep
Total	245.65	252.52	232.09
Combined water	169.23	125.93	115.27
Hemicellulose	186.05	216.56	191.38
Cellulose	177.98	187.37	179.14
Lignin	221.53	236.97	174.50

description of the dominant gaseous-evolution behavior of the three coconut residues[14,20,23]. In addition, compared with many other low-*m*/*z* fragment ions, these three signals are more suitable for comparative analysis of overall devolatilization trends because their interpretation is relatively straightforward and their relevance to biomass oxygen-release behavior is better established in the literature[14,20]. Although other fragment ions may also contain useful information, they were not discussed in detail here because many low-*m*/*z* organic fragments may have overlapping assignments, whereas *m*/*z* = 18, 28, and 44 serve as more robust indicators of the main gaseous-evolution behavior under the present analytical objective.

For the ion fragment with *m*/*z* = 18 (corresponding to H_2O), the signal intensity of combined water released during the pyrolysis of coconut coir is significantly higher than that of the other two residues. This can be primarily attributed to the higher cellulose content in coconut coir (as shown in Fig. 4b), which possesses a

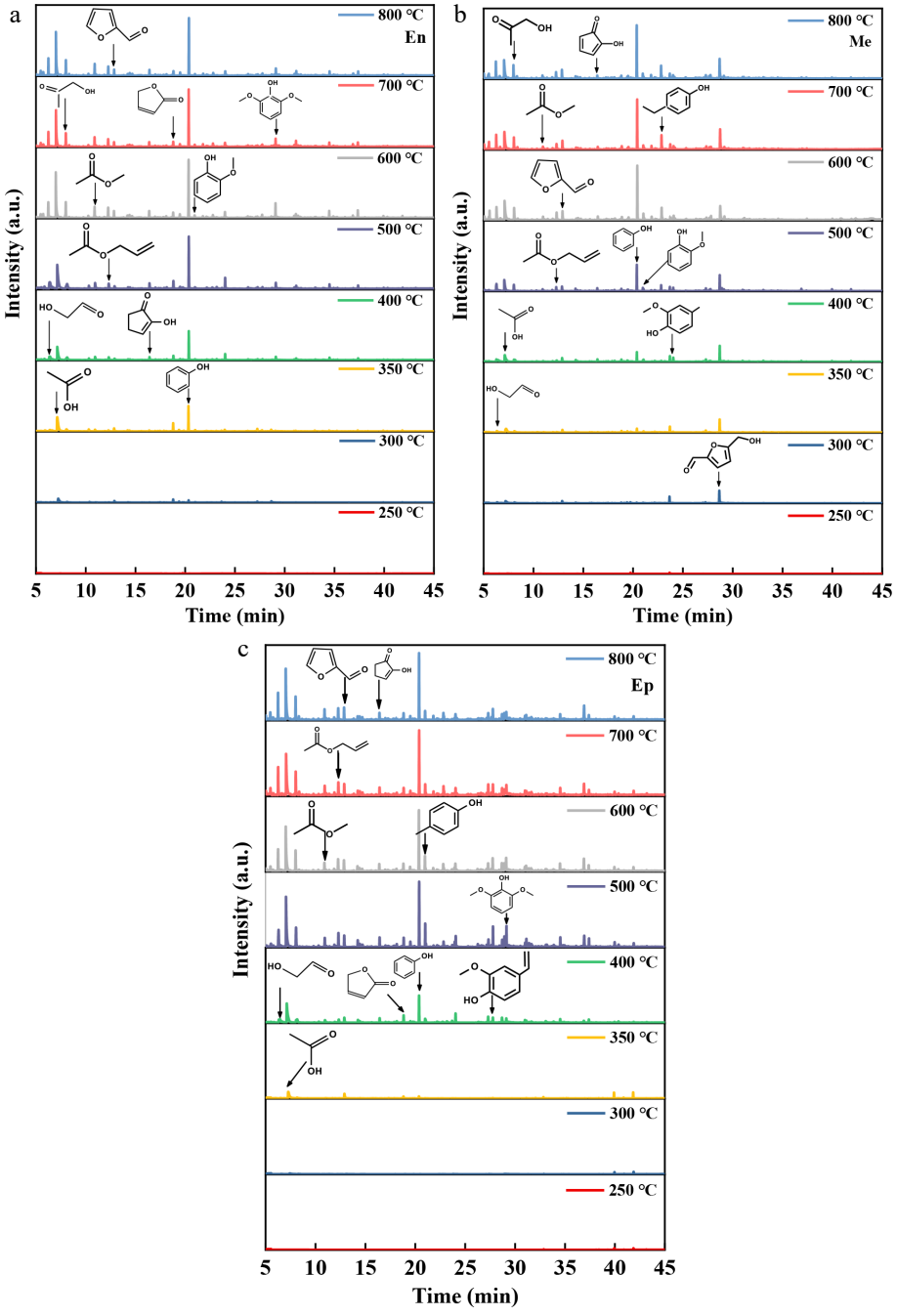

Fig. 4 The gas chromatogram spectra for fast pyrolysis products of (a) coconut shell (En), (b) coir (Me), and (c) husk (Ep) at different temperatures.

https://doi.org/10.48130/prkm-0026-0015

stronger water-holding capacity[20]. The signal intensities for m/z = 28 and m/z = 44 (corresponding to CO and CO_2, respectively) are similar among the coconut wastes, with the signal peaks appearing in the temperature range of 300–500 °C. This temperature range corresponds to the formation stage of carbon-containing volatile components during the pyrolysis process[23].

Py-GC/MS analysis

The chromatograms of the pyrolysis products from 250 to 800 °C are shown in Fig. 4. As shown in Fig. 4, volatile products dominated by acids, aldehydes, and phenols are generated from the pyrolysis of all three feedstocks as the temperature increases. Acetic acid, furfural, hydroxyacetaldehyde, 2(5H)-furanone, 5-hydroxymethylfurfural, and hydroxyacetone are all typical pyrolysis products of cellulose and hemicellulose. Phenolic compounds such as phenol, 2-methoxy-4-methylphenol, and 2,6-dimethoxyphenol are typical pyrolysis products of lignin[14]. The temperature and source of these products correspond well with the TG/DTG curves, further confirming that the second, third, and fourth Gaussian-fitted peaks in the main pyrolysis stage correspond to hemicellulose, cellulose, and lignin, respectively.

Phenolic products obtained from Py-GC/MS can be used to infer lignin structural features in the feedstock. In general, lignin is commonly categorized as softwood-type (primarily guaiacyl-derived structures), hardwood-type (containing both guaiacyl- and syringyl-derived structures), and grass-type (containing guaiacyl-, syringyl-, and p-hydroxyphenyl-derived structures)[24]. In this study, the lignin-type inference was made qualitatively based on representative diagnostic phenolic compounds in Fig. 4. Specifically, guaiacol was used as a diagnostic indicator of guaiacyl-derived structures, 2,6-dimethoxyphenol as a diagnostic indicator of syringyl-derived structures[25], and p-cresol as a diagnostic indicator associated with p-hydroxyphenyl-derived structures. Guaiacol was detected in all three feedstocks; 2,6-dimethoxyphenol was observed in coconut shell and husk; and p-cresol was only detected in coconut husk. Based on the presence/absence patterns of these diagnostic phenolic markers, the lignin in coconut shell, coir, and husk was therefore identified as predominantly hardwood-type, softwood-type, and grass-type, respectively. It should be noted that this classification provides a qualitative compositional indication and may be influenced by secondary reactions during pyrolysis; therefore, the term 'predominantly' is used throughout.

In addition to the lignin structural differences revealed by phenolic products, the synergistic effect of pyrolysis temperature and feedstock chemical composition exerts a more profound influence on the distribution of volatile products, as illustrated in Fig. 5. To further evaluate the potential influence of producing region on pyrolysis product distribution, supplementary Py-GC/MS analyses were conducted on coconut shell, coir, and husk samples collected from several distinct coconut-producing regions in China under the same pretreatment and experimental conditions as those used in the main study. The product-distribution results at 600 °C for samples collected from Guangdong, Guangxi, and the tropical areas of Southern Yunnan are shown in Supplementary Fig. S4. Compared with the results presented in Fig. 5, the additional samples exhibited highly similar product categories and temperature-dependent evolution trends. The relative deviations in the major product distributions among different producing regions were within 5%, which is within the experimental uncertainty of the present Py-GC/MS measurements. These results indicate that, under the present experimental conditions, the influence of the producing region on the overall product distribution is limited. Therefore, the pyrolysis product distributions of the three main feedstocks discussed below can still be considered representative and composition-dependent. Among all feedstocks, acids (primarily acetic acid) show the highest relative content at 400 °C, which is mainly attributed to the low-temperature cleavage of acetyl groups in hemicellulose[20]. Notably, although the hemicellulose content of coconut coir has been confirmed to be lower than that of the other two feedstocks, it produces the highest proportion of aldehydes at 400 °C. This is consistent with its higher cellulose content, as aldehydes (such as furfural and hydroxyacetaldehyde) are typical primary products of cellulose pyrolysis[26]. As the temperature rises to 500 °C and above, the relative contents of both acids and aldehydes generally decrease across all feedstocks, indicating that these primary products undergo further secondary cracking or dehydration reactions at higher temperatures.

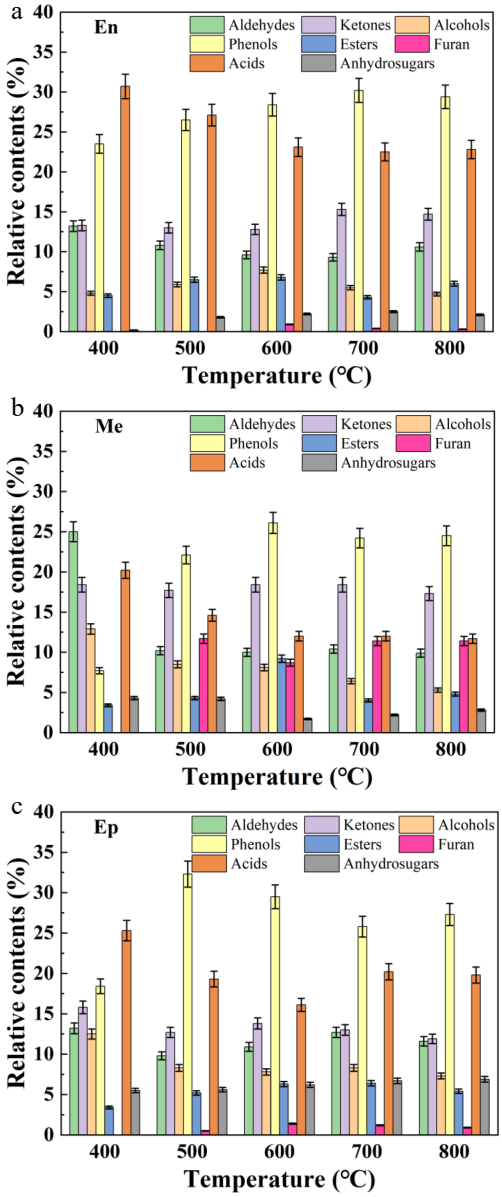

Fig. 5 Distribution of fast pyrolysis products from (a) coconut shell (En), (b) coir (Me) and (c) husk (Ep) at different temperatures.

However, the three feedstocks exhibit significant divergence in key product evolution pathways, which directly corroborates their

composition-dominated pyrolysis mechanisms. For coconut shell, which contains the highest proportion of hardwood lignin, its pyrolysis products are consistently characterized by a high proportion of phenols, showing a steadily increasing trend with rising temperature. This indicates that its dense lignin structure can be continuously and effectively depolymerized throughout the tested temperature range[27]. In contrast, the most prominent feature in the product distribution of coconut coir is the exceptionally high selectivity toward furan compounds (such as furan and methylfuran) after 500 °C, far exceeding that of the other two feedstocks. This phenomenon may originate from its cellulose-dominated pyrolysis pathway: the pyran rings of cellulose units can undergo ring-opening, C–C bond cleavage, and secondary deoxygenation reactions during pyrolysis, directly yielding simple furan ring structures[28]. Although the hemicellulose content in coconut coir is relatively low, its specific hemicellulose components may also contribute to the formation of furan compounds. The loose physical structure of coconut coir may further facilitate the rapid release of volatile products, suppressing secondary reactions of furan compounds, and thereby enhancing their selectivity[29]. This unique product distribution positions coconut coir as a potential high-quality feedstock for recovering furan-based platform chemicals.

Furthermore, coconut husk exhibits another distinctive characteristic: a relatively high proportion of acid products at lower temperatures, together with a clear temperature-dependent evolution of product distribution. This behavior may be associated with the synergistic effects between its relatively high hemicellulose content and its grass-type lignin structure[30]. The preferential depolymerization of hemicellulose at relatively low temperatures releases a large amount of organic acids such as acetic acid, which can establish a localized acidic catalytic environment during the subsequent main pyrolysis stage of cellulose. Such an environment may promote the cleavage of cellulose glycosidic bonds while inhibiting competing pathways, such as ring-opening reactions that form small-molecule aldehydes or further conversion to furans, thereby affecting the formation of characteristic oxygenated products, including anhydrosugars such as levoglucosan[31]. Additionally, the unique grass-type lignin structure, containing p-hydroxyphenyl units, may also form specific cross-links with the cellulose/hemicellulose components, collectively influencing the pyrolysis pathway of coconut husk[20]. Therefore, the product distribution of coconut husk should be described in a temperature-dependent manner rather than by stating that one product category dominates at all temperatures.

When the temperature exceeds 700 °C, secondary reactions become more significant. The decrease in acid content and the emergence of trace amounts of aliphatic and aromatic hydrocarbons (all below 1.5%) in all feedstocks are attributed to reactions such as decarboxylation, decarbonylation, and aromatization of oxygen-containing compounds (e.g., acids and aldehydes). However, even at 800 °C, hydrocarbon yields remain extremely low, indicating that deep deoxygenation pathways leading to hydrocarbon formation are not dominant under fast pyrolysis conditions.

In summary, Py-GC/MS analysis not only confirms the chemical composition differences of the three coconut by-products, as inferred from TG/DTG curves and chemical analysis, but more importantly, reveals their unique thermochemical conversion pathways. These pathways are co-determined by their chemical compositions and the interactions among the components. The hardwood lignin in coconut shell serves as a stable source of phenolic compounds; coconut coir, owing to its cellulose-dominated deep deoxygenation pathway, acts as a high-yield feedstock for furan compounds; while coconut husk demonstrates significant potential for producing anhydrosugars, likely due to synergistic catalysis induced by its higher hemicellulose content and grass lignin. These findings provide a crucial scientific basis for the targeted pyrolysis valorization of coconut waste based on different desired products.

Kinetic analysis

In order to study the pyrolysis kinetics of coconut husk wastes comprehensively, the apparent activation energy of coconut waste is obtained by using isoconversion and Gaussian fitting-isoconversional methods. The results are compared and analyzed to obtain more details of the pyrolysis process. The conversion degree (α) was evaluated over the range of 0.05–0.95 with an increment of 0.05 (step size ≤ 0.05) following the International Confederation for Thermal Analysis and Calorimetry (ICTAC) Kinetics Committee recommendations. The endpoint regions ($\alpha < 0.05$ and $\alpha > 0.95$) were excluded to minimize baseline uncertainty and experimental noise near the extremes[32]. The Starink method was applied to the non-isothermal data, with the linear fitting results confirming the high reliability of the model ($R^2 > 0.96$) for all three samples (Supplementary Fig. S5). The E_a profiles derived from the isoconversional method (Supplementary Fig. S6) revealed three distinct stages, which correspond well with the thermal decomposition behavior observed in the TG/DTG curves. The initial stage (α = 0.05~0.35) exhibited a gradual increase in E_a, indicative of the progressive decomposition of the less stable hemicellulose and the initiation of cellulose degradation. Within the primary devolatilization zone (α = 0.35~0.60), a slight decrease or plateau in E_a was observed, suggesting accelerated reactions due to synergistic interactions between the biomass components. The final stage (α = 0.60~0.95) was characterized by a rapid rise in E_a, reflecting the dominant carbonization reactions of lignin, which require higher energy inputs for condensation and rearrangement processes.

The Gaussian deconvolution of the DTG curves (Fig. 3) enabled a more precise attribution of the apparent activation energy to the components (combined water, hemicellulose, cellulose, and lignin), as shown in Supplementary Fig. S7. The calculated E_a values for each component are summarized in Table 2. These data provide critical insights into the interactions between components. For cellulose, the activation energies of the three feedstocks are relatively close (177.98–187.37 kJ/mol), suggesting that the intrinsic thermal decomposition behavior of cellulose remains comparatively stable among the three coconut wastes. Nevertheless, the slightly higher cellulose activation energy observed for coconut coir may reflect differences in the surrounding matrix environment. In particular, variations in the contents and structural characteristics of hemicellulose and lignin may influence the local reaction environment through different catalytic or inhibitory effects during the main cellulose-decomposition stage. Because the component-wise activation energies in this study were derived from deconvolution-based kinetic analysis rather than from multiple independent statistical replicates, these differences should not be overinterpreted as statistically significant. Instead, they are interpreted as moderate but mechanistically meaningful variations that are consistent with differences in feedstock composition and component interactions.

The activation energies for hemicellulose decomposition in coconut shell and coconut husk (186.05 and 191.38 kJ/mol, respectively) are lower than that of coconut coir (216.56 kJ/mol). This difference may be primarily attributed to the acid-catalyzed self-promoting effect of acetic acid released during hemicellulose pyrolysis. Acetic acid is a typical primary product formed from the cleavage of acetyl groups in hemicellulose, and once released *in situ*, it can contribute to a localized acidic environment that promotes the

https://doi.org/10.48130/prkm-0026-0015

cleavage of glycosidic bonds and side chains, thereby facilitating further hemicellulose decomposition. In this sense, the process is described here as autocatalytic, because a product generated during the early-stage decomposition of hemicellulose can in turn promote the subsequent degradation of the same component. Therefore, the lower apparent activation energies observed for coconut shell and coconut husk are considered to be consistent with a stronger *in-situ* acid-promoting effect than in coconut coir, which contains less hemicellulose and correspondingly releases less acetic acid[14,20,33]. As shown by the Py-GC/MS results (Fig. 5), coconut shell and husk, which have higher hemicellulose contents, release a larger amount of acetic acid during the initial stage of pyrolysis. Acting as an acidic catalyst, acetic acid effectively promotes the cleavage of glycosidic bonds and side chains in hemicellulose, thereby lowering its apparent decomposition energy barrier. In contrast, coconut coir has the lowest hemicellulose content, resulting in insufficient acid release during pyrolysis and a weak autocatalytic effect. Consequently, its hemicellulose pyrolysis more closely resembles a non-catalytic homogeneous reaction, exhibiting a higher activation energy.

For lignin pyrolysis, coconut husk exhibits the lowest activation energy (174.50 kJ/mol), while coconut shell and coconut coir show higher values (221.53 and 236.97 kJ/mol, respectively). This trend is consistent with the Py-GC/MS results, where the husk sample exhibits distinctive lignin-derived product evolution over a wide temperature range. The difference is not attributed to lignin type alone, but may also reflect the combined effects of lignin interunit linkage characteristics and structural heterogeneity[34], as well as interactions with surrounding carbohydrate components[35]. In particular, grass-type lignin containing p-hydroxyphenyl units may possess different bond distributions and decomposition characteristics from hardwood- and softwood-type lignin, which can affect its thermal stability and cleavage behavior[34,36]. In addition, lignin–carbohydrate interactions and volatile intermediates generated from hemicellulose and cellulose pyrolysis may further modify the local reaction environment and promote lignin decomposition[35]. Notably, the activation energies of the lignin component in all three feedstocks are lower than those commonly reported for isolated lignin (approximately 250–300 kJ/mol), suggesting that the pyrolysis of surrounding carbohydrates contributes to the apparent synergistic promotion of lignin degradation[35].

Figure 6 provides a more intuitive perspective for understanding the pyrolysis process through the activation energy–temperature relationship. By comparing the calculation results of the isoconversional (Iso) method and the Gaussian fit-isoconversional method across different temperature intervals, the variations in the energy barriers for the decomposition of different components and their dependence on temperature can be clearly observed.

Overall, the general trends derived from the two calculation methods are similar, but the Gaussian fit-isoconversional method more accurately reflects the decomposition behavior of each component within specific temperature intervals. In the 200~300 °C range, corresponding to the main decomposition stage of hemicellulose, the activation energies of coconut shell and husk are significantly lower than that of coconut coir, which is fully consistent with the aforementioned acetic acid autocatalytic mechanism. Notably, a

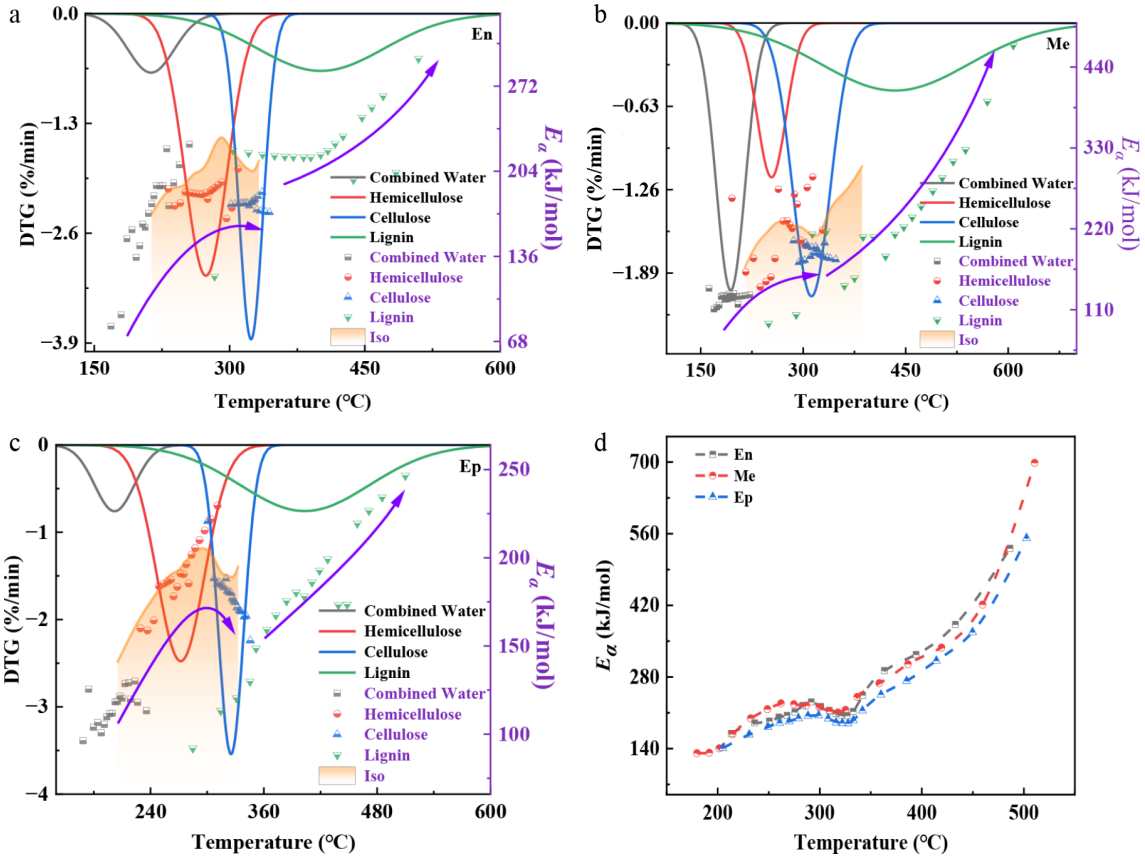

Fig. 6 Activation energy curves with temperature. Comparison of the results of each component of (a) coconut shell (En), (b) coir (Me), and (c) husk (Ep) with the isoconversional method in the reference interval. (d) Comparison of the results of the isoconversional method within the intact intervals of En, Me, and Ep.

distinct peak in the activation energy for hemicellulose decomposition of coconut coir is observed around 225 °C. This is directly related to its compositional characteristic of having the lowest hemicellulose content; the lower abundance of precursors results in insufficient total acetic acid released during pyrolysis and a weak autocatalytic effect. Consequently, the decomposition of its hemicellulose relies more on thermal energy itself, exhibiting a higher activation energy barrier at the main reaction temperature[37].

In the 300~400 °C range, which corresponds to the main decomposition stage of cellulose, the activation energy curves of all three feedstocks display relatively flat characteristics. However, the activation energy of coconut coir in this range is slightly higher than that of the other two feedstocks, which may be related to more concentrated volatile release due to its high cellulose content[38]. For the lignin decomposition stage above 400 °C, the activation energy of coconut husk remains at a relatively low level and increases slowly with rising temperature, further confirming the thermal instability of its grass lignin structure. In contrast, the activation energies for lignin decomposition in coconut shell and coir rise sharply in the high-temperature region, especially for coconut coir, where the lignin activation energy exceeds 300 kJ/mol, reflecting the higher energy required to break the recalcitrant C–C bonds in its softwood lignin structure[39].

Conclusions

This study systematically elucidated the distinct pyrolysis pathways of three coconut wastes (coconut shell, coir, and husk) by correlating product distributions from Py-GC/MS with kinetic parameters derived from the Gaussian fit-isoconversional method. Coconut coir, which is rich in cellulose, exhibited high selectivity toward furans, whereas coconut shell and coconut husk showed greater tendencies toward phenolic and acid products, respectively. Kinetic analysis further revealed that the *in situ*-formed acetic acid from hemicellulose could autocatalytically lower its decomposition energy barrier. The activation energy for lignin pyrolysis was the lowest in coconut husk containing grass lignin (174.50 kJ/mol), and the lignin-related activation energies in all three samples were lower than those reported for isolated lignin (250–300 kJ/mol), demonstrating catalytic synergy from surrounding carbohydrates. Overall, the present study shows that the pyrolysis behavior of coconut wastes is strongly governed by feedstock composition and component interactions. Coconut shell is more suitable for phenolic-oriented valorization, coconut coir shows greater potential for furan-oriented utilization, and coconut husk is more favorable for acid-oriented conversion. These findings provide fundamental insights into composition-dependent reaction mechanisms and offer a useful basis for the targeted valorization of different coconut waste streams into specific bio-based chemicals.

Author contributions

The authors confirm their contributions to the paper as follows: study conception and design: Yuan H; data collection: Yu Q, Shan R; analysis and interpretation of results: Li Z; draft manuscript preparation: Li C, Zhang J. All authors reviewed the results and approved the final version of the manuscript.

Data availability

The data that support the findings of this study are available upon reasonable request from the corresponding author.

Acknowledgments

This work was supported by the National Natural Science Foundation of China (52506288, 52276219), the Project of Science and Technology of Guangzhou (2025A04J5365), and the Youth Innovation Promotion Association CAS (2023367).

Conflict of interest

The authors declare that they have no conflict of interest.

Supplementary information accompanies this paper online at: https://doi.org/10.48130/prkm-0026-0015.

Dates

Received 31 December 2025; Revised 25 April 2026; Accepted 13 May 2026; Published online 29 July 2026

References

[1] Poornima S, Manikandan S, Prakash R, Deena SR, Subbaiya R, et al. 2024. Biofuel and biochemical production through biomass transformation using advanced thermochemical and biochemical processes – a review. *Fuel* 372:132204

[2] Cheng C, Ding L, Guo Q, He Q, Gong Y, et al. 2022. Process analysis and kinetic modeling of coconut shell hydrothermal carbonization. *Applied Energy* 315:118981

[3] Azeta O, Ayeni AO, Agboola O, Elehinafe FB. 2021. A review on the sustainable energy generation from the pyrolysis of coconut biomass. *Scientific African* 13:e00909

[4] Ighalo JO, Conradie J, Ohoro CR, Amaku JF, Oyedotun KO, et al. 2023. Biochar from coconut residues: an overview of production, properties, and applications. *Industrial Crops and Products* 204:117300

[5] Suman S, Gautam S. 2017. Pyrolysis of coconut husk biomass: analysis of its biochar properties. *Energy Sources, Part A: Recovery, Utilization, and Environmental Effects* 39:761–767

[6] Ahmad RK, Sulaiman SA, Inayat M, Umar HA. 2020. The effects of temperature, residence time and particle size on a charcoal produced from coconut shell. *IOP Conference Series: Materials Science and Engineering* 863:012005

[7] Akter MM, Surovy IZ, Sultana N, Faruk MO, Gilroyed BH, et al. 2024. Techno-economics and environmental sustainability of agricultural biomass-based energy potential. *Applied Energy* 359:122662

[8] Monir MU, Khatun F, Abd Aziz A, Vo DVN. 2020. Thermal treatment of tar generated during co-gasification of coconut shell and charcoal. *Journal of Cleaner Production* 256:120305

[9] Sarkar JK, Wang Q. 2020. Different pyrolysis process conditions of South Asian waste coconut shell and characterization of gas, bio-char, and bio-oil. *Energies* 13:1970

[10] Romero Millán LM, Sierra Vargas FE, Nzihou A. 2021. Characterization of steam gasification biochars from lignocellulosic agrowaste towards soil applications. *Waste and Biomass Valorization* 12:4141–4155

[11] Ma Z, Wang J, Yang Y, Zhang Y, Zhao C, et al. 2018. Comparison of the thermal degradation behaviors and kinetics of palm oil waste under nitrogen and air atmosphere in TGA-FTIR with a complementary use of model-free and model-fitting approaches. *Journal of Analytical and Applied Pyrolysis* 134:12–24

[12] Ma Z, Sun Q, Ye J, Yao Q, Zhao C. 2016. Study on the thermal degradation behaviors and kinetics of alkali lignin for production of phenolic-rich bio-oil using TGA–FTIR and Py–GC/MS. *Journal of Analytical and Applied Pyrolysis* 117:116–124

[13] Kazawadi D, Ntalikwa J, Kombe G. 2022. Co-pyrolysis of cashew nut, coconut shells, and rice husk waste: kinetic and thermodynamic investigations. *Energy Sources, Part A: Recovery, Utilization, and Environmental Effects* 44:5896–5915

https://doi.org/10.48130/prkm-0026-0015

[14] Wang S, Dai G, Yang H, Luo Z. 2017. Lignocellulosic biomass pyrolysis mechanism: a state-of-the-art review. *Progress in Energy and Combustion Science* 62:33–86
[15] Lopes FCR, Tannous K. 2020. Coconut fiber pyrolysis decomposition kinetics applying single- and multi-step reaction models. *Thermochimica Acta* 691:178714
[16] Li C, Zhang J, Shan R, Yuan H, Chen Y. 2023. Kinetic study for thermocatalytic degradation of waste mixed cloth over antibiotic residue derived carbon-based solid acids. *Fuel* 331:125797
[17] Starink MJ. 2003. The determination of activation energy from linear heating rate experiments: a comparison of the accuracy of isoconversion methods. *Thermochimica Acta* 404:163–176
[18] Sokoto MA, Singh R, Krishna BB, Kumar J, Bhaskar T. 2016. Non-isothermal kinetic study of de-oiled seeds cake of African star apple (*Chrosophyllum albidum*) using thermogravimetry. *Heliyon* 2:e00172
[19] Rueda-Ordóñez YJ, Arias-Hernández CJ, Manrique-Pinto JF, Gauthier-Maradei P, Bizzo WA. 2019. Assessment of the thermal decomposition kinetics of empty fruit bunch, kernel shell and their blend. *Bioresource Technology* 292:121923
[20] Yang H, Yan R, Chen H, Lee DH, Zheng C. 2007. Characteristics of hemicellulose, cellulose and lignin pyrolysis. *Fuel* 86:1781–1788
[21] Alabi AO, Sambo AS. 2023. Comparative bio-energy potential of De-oiled coconut pulp and Coconut shell: insights from physicochemical characterization, pyrolysis kinetics and thermodynamic studies. *Fuel Processing Technology* 243:107658
[22] Rueda-Ordóñez YJ, Tannous K. 2018. Drying and thermal decomposition kinetics of sugarcane straw by nonisothermal thermogravimetric analysis. *Bioresource Technology* 264:131–139
[23] Liu Q, Wang S, Zheng Y, Luo Z, Cen K. 2008. Mechanism study of wood lignin pyrolysis by using TG–FTIR analysis. *Journal of Analytical and Applied Pyrolysis* 82:170–177
[24] Zakzeski J, Bruijnincx PCA, Jongerius AL, Weckhuysen BM. 2010. The catalytic valorization of lignin for the production of renewable chemicals. *Chemical Reviews* 110:3552–3599
[25] Li C, Zhao X, Wang A, Huber GW, Zhang T. 2015. Catalytic transformation of lignin for the production of chemicals and fuels. *Chemical Reviews* 115:11559–11624
[26] Staš M, Auersvald M, Kejla L, Vrtiška D, Kroufek J, et al. 2020. Quantitative analysis of pyrolysis bio-oils: a review. *TrAC Trends in Analytical Chemistry* 126:115857
[27] Bianasari AA, Le MT, Abu Bakar MS, Saepurahman, Mansur D, et al. 2026. Phenol-rich bio-oil synthesis via single and dual metal-oxide/zeolite catalysts in biomass catalytic pyrolysis: comparison of Y_2O_3/ZSM-5 and MgO/Y_2O_3/ZSM-5. *Biomass and Bioenergy* 205:108565
[28] Ali I, Bahaitham H, Naebulharam R. 2017. A comprehensive kinetics study of coconut shell waste pyrolysis. *Bioresource Technology* 235:1–11
[29] Gao Y, Yang Y, Qin Z, Sun Y. 2016. Factors affecting the yield of bio-oil from the pyrolysis of coconut shell. *SpringerPlus* 5:333
[30] Hubble AH, Goldfarb JL. 2021. Synergistic effects of biomass building blocks on pyrolysis gas and bio-oil formation. *Journal of Analytical and Applied Pyrolysis* 156:105100
[31] Li X, Cen K, Li J, Jia D, Gao J, et al. 2025. Insights into the interactions between cellulose and hemicellulose during pyrolysis for optimizing the properties of biochar as a potential energy vector. *Industrial Crops and Products* 223:120126
[32] Vyazovkin S, Burnham AK, Criado JM, Pérez-Maqueda LA, Popescu C, et al. 2011. ICTAC Kinetics Committee recommendations for performing kinetic computations on thermal analysis data. *Thermochimica Acta* 520:1–19
[33] Yang X, Zhao Y, Li W, Li R, Wu Y. 2019. Unveiling the pyrolysis mechanisms of hemicellulose: experimental and theoretical studies. *Energy & Fuels* 33:4352–4360
[34] Suota MJ, da Silva TA, Zawadzki SF, Sassaki GL, Hansel FA, et al. 2021. Chemical and structural characterization of hardwood and softwood LignoForce™ lignins. *Industrial Crops and Products* 173:114138
[35] Siddiqi H, Kumari U, Biswas S, Mishra A, Meikap BC. 2020. A synergistic study of reaction kinetics and heat transfer with multi-component modelling approach for the pyrolysis of biomass waste. *Energy* 204:117933
[36] Akazawa M, Kojima Y, Kato Y. 2016. Effect of pyrolysis temperature on the pyrolytic degradation mechanism of β-aryl ether linkages. *Journal of Analytical and Applied Pyrolysis* 118:164–174
[37] Gorshkov A, Berezikov N, Kaltaev A, Yankovsky S, Slyusarsky K, et al. 2021. Analysis of the physicochemical characteristics of biochar obtained by slow pyrolysis of nut shells in a nitrogen atmosphere. *Energies* 14:8075
[38] Wu Y, Gui Q, Zhang H, Li H, Li B, et al. 2023. Effect of biomass components' interaction on the pyrolysis reaction kinetics and small-molecule product release characteristics. *Journal of Analytical and Applied Pyrolysis* 173:106039
[39] Ding K, Wang Y, Liu S, Lin G, Syed-Hassan SSA, et al. 2021. Volatile-char interactions during biomass pyrolysis: insight into the activity of chars derived from three major components. *Journal of Analytical and Applied Pyrolysis* 159:105320

Copyright: © 2026 by the author(s). Published by Maximum Academic Press, Fayetteville, GA. This article is an open access article distributed under Creative Commons Attribution License (CC BY 4.0), visit https://creativecommons.org/licenses/by/4.0/.